

# Preclinical Evaluation of a Microtubule PET Ligand [<sup>11</sup>C]MPC-6827 in Tau and Amyotrophic Lateral Sclerosis Animal Models

J. S. Dileep Kumar<sup>1,2\*</sup>, Andrei Molotkov<sup>3</sup>, Jongho Kim<sup>3</sup>, Patrick Carberry<sup>3</sup>, Sidney Idumonyi<sup>3</sup>, John Castrillon<sup>3</sup>, Karen Duff<sup>4,5</sup>, Neil A. Shneider<sup>6</sup>, Akiva Mintz<sup>1,3</sup>

<sup>1</sup>Division of Molecular Imaging and Neuropathology, New York State Psychiatric Institute, New York; <sup>2</sup>Feinstein Institutes for Medical Research, North Shore University Hospital, Manhasset, New York, <sup>3</sup>Department of Radiology, Columbia University Medical Center, New York; <sup>4</sup>Department of Pathology and Cell Biology & Taub Institute, Columbia University Medical Center; <sup>5</sup>UK Dementia Research Institute, University College London, UK; <sup>6</sup>Department of Neurology and Eleanor and Lou Gehrig ALS Center, Columbia University Medical Center, New York

\*Corresponding author (current address):

J. S. Dileep Kumar, PhD, Feinstein Institutes for Medical Research, North Shore University Hospital, Manhasset, New York, USA.

Email: dkumar7@northwell.edu

Running title: Preclinical Evaluation of [<sup>11</sup>C]MPC-6827 in tau and ALS animal models

## Abstract

**Background:** Microtubules are abundant in brain and their malfunctioning occurs in the early to advanced stages of neurodegenerative disorders. At present there is no *in vivo* test available for a definitive diagnosis of most of the neurodegenerative disorders. Herein, we present the microPET imaging of microtubules using our recently reported Positron Emission Tomography (PET) tracer, [<sup>11</sup>C]MPC-6827, in transgenic mice models of tau pathology (rTg4510) and amyotrophic lateral sclerosis pathology (SOD1\*G93A) and compared to corresponding age matched controls.

**Methods:** Automated synthesis of [<sup>11</sup>C]MPC-6827 was achieved in a GE-FX2MeI/FX2M radiochemistry module. *In vivo* PET imaging studies of [<sup>11</sup>C]MPC-6827 (3.7±0.8 MBq) were performed in rTg4510 and SOD1\*G93A mice groups and their corresponding littermates (n=5 per group). Dynamic PET images were acquired using a microPET Inveon system (Siemens, Germany) at 55 minutes for rTg4510 and 30 minutes for SOD1\*G93A and corresponding controls. PET images were reconstructed using the 3D-OSEM algorithm and analyzed using VivoQuant version 4 (Invicro, MA). Tracer uptake in ROIs that included whole brain was measured as %ID/g over time to generate standardized uptake values (SUV) and time-activity curves (TACs).

**Results:** [<sup>11</sup>C]MPC-6827 exhibit a trend of lower tracer binding in mouse models of Alzheimer's disease (tau pathology, line rTg4510) and Amyotrophic Lateral Sclerosis (line SOD1\*G93A) compared to wild type littermates.

**Conclusions:** Our finding indicates a trend of loss of microtubule binding of [<sup>11</sup>C]MPC-6827 in the whole brain of AD and ALS transgenic mice models compared to control mice. The pilot studies described herein show that [<sup>11</sup>C]MPC-6827 could be used as a PET ligand for preclinical and human brain imaging of Alzheimer's disease, ALS and other neurodegenerative diseases.

Keywords: Microtubule, PET, Alzheimer's disease, Amyotrophic Lateral Sclerosis

## **Abbreviations**

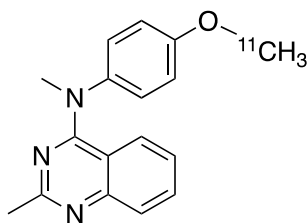
A $\beta$	Amyloid beta
AD	Alzheimer's Disease
ALS	Amyotrophic Lateral Sclerosis
BBB	Blood brain barrier
CNS	Central nervous system
FTD	Frontotemporal lobe dementia
ID/g	injected dose/gram
LTP	Long-term potentiation
MAP	Microtubule associated protein
MBq	Mega becquerel
MT	Microtubule
MTA	Microtubule targeting agent
ND	Neurodegenerative disorder
NFT	Neurofibrillary tangles
PET	Positron Emission Tomography
PTM	Post-translational modifications
TAC	time activity curves
SEM	Standard error of the mean
SUV	standardized uptake value
VOI	Volume of interest

## **Introduction**

Neurodegenerative disorders (NDs) are highly prevalent brain diseases among the aging population, and no definitive cures exist [1-3]. Appropriate biomarkers are not available to diagnose NDs at an early stage, and it may be far too late to treat the disease effectively after symptoms appear. Although neurodegeneration is considered to be a major pathology, the causes and mechanisms underlying brain abnormalities in NDs are not yet fully understood. Therefore, the development and validation of a unique neuroimaging biomarker for NDs that identifies a common pathogenic mechanism of neurodegeneration should be a top research priority. There is currently no validated PET ligand available for imaging and tracking the degeneration process in NDs. Such an agent would be useful for both clinical early diagnoses, prior to the emergence of clinical symptoms, as well as a tool for preclinical studies of NDs.

Abnormalities in microtubule (MT) dynamics are positively associated with neurodegeneration and they have been characterized as a validated biomarker for a variety of sporadic and familial NDs [4-6]. Neurodegeneration is often associated with axonal swellings, axonal transport deficit, and the accumulation of proteins [7-9]. These symptoms have been associated with alterations of the cytoskeleton, and a large body of literature links MT dysfunction leading to neurodegeneration in early to advanced stages of NDs [4-6]. For all the above reasons, MTs are promising targets for pharmacological treatment as well as a biomarker for NDs. NDs associated with tau pathology (collectively known as tauopathies) including Alzheimer's disease (AD) and frontotemporal lobe dementia linked to tau (FTD-tau) are the best-documented diseases with MT pathophysiology in the central nervous system (CNS). This likely occurs as tau is a microtubule associated protein (MAP) and, under pathological conditions, MAP dissociates from MTs, most likely as a result of hyperphosphorylation [4-6]. Similarly, severe dysfunction of MT dynamics is reported in Amyotrophic Lateral Sclerosis (ALS) [10-12]. Although the exact mechanisms underlying MT dysfunction in ALS are not established yet, aberrant alterations in MT dynamics resulting in dysregulated axonal transport are thought to drive cytoskeletal and cellular abnormalities leading to disease progression [13]. Therefore, modulation of MT associated events and MT structural

integrity is an attractive therapeutic target and an *in vivo* biomarker for NDs. For AD, we predict that a MT-based PET tracer will provide a higher signal to noise ratio compared to tau and  $\beta$ -amyloid ( $A\beta$ ) targeted PET tracers as in addition to  $A\beta$  and tau, a number of mutated proteins and post translational modifications (PTM) also contribute to MT loss in AD and a variety of NDs [4-6]. The accumulation of tau and  $A\beta$  proteins likely represent only a subset of MT-associated abnormalities present in the degenerating AD brain. Previous generations of PET radiotracers reported for MT tracers did not show much uptake in the brain because these tracers are well-characterized substrates of efflux transporters [14]. We screened many microtubule targeting agents (MTAs) as potential PET imaging tracers for MTs and our lead radiotracer [ $^{11}\text{C}$ ]MPC-6827 exhibits high blood brain barrier (BBB) penetration, retention and specific binding in rodent brain (Figure 1) [15, 16]. Our pilot preclinical PET imaging studies of [ $^{11}\text{C}$ ]MPC-6827 show a trend of lower binding in whole brain and prefrontal cortex of chronic ethanol treated mice compared to water treated control group [17]. Here we report results describing the preclinical imaging of [ $^{11}\text{C}$ ]MPC-6827 in transgenic mouse models with tau pathology (rTg4510) or ALS (SOD1\*G93A) compared to corresponding age matched controls [18, 19].



## Materials and methods

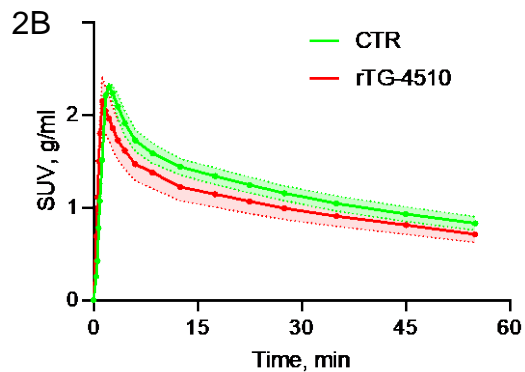
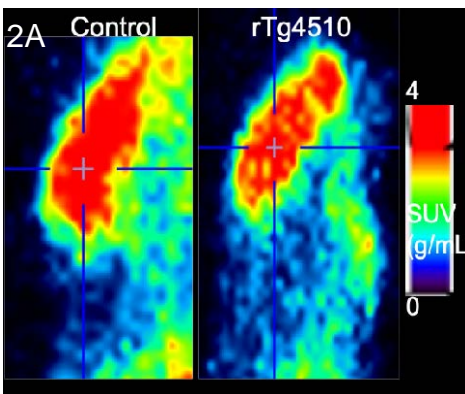
Radiosynthesis of [ $^{11}\text{C}$ ]MPC-6827 was performed using our previously established procedure [15-17]. All animal experiments were carried out with the approval of the Institutional Animal Care and Use Committees (IACUC) of Columbia University Medical Center (CUMC). Mouse lines rTg4510 (9-month-old) and SOD1\*G93A (2-month-old) and their corresponding age-matched littermates were originally obtained from Jackson laboratories and bred and maintained at CUMC [18, 19]. Dynamic microPET scans (30 or 55 min) were performed on a Siemens Inveon microPET after tail vein administration of [ $^{11}\text{C}$ ]MPC-6827 ( $1.85 \pm 0.37$  MBq, 200  $\mu\text{L}$  volume) [17]. Image analyses were

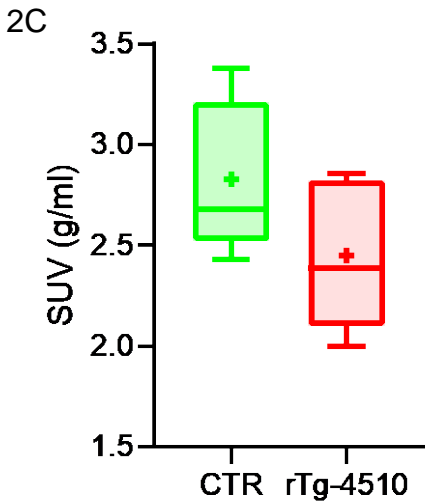
performed using VivoQuant (version 4, Invivo, MA) software. The time activity curves (TACs) and standardized uptake values (SUV) were derived from three-dimensional ellipsoid volume of interests (VOIs) ranging from 2-6 mm<sup>3</sup> placed manually at the center of the brain VOIs.

### Statistical analyses

Time activity curves are as mean  $\pm$  standard error of the mean (SEM), unless otherwise stated. Since the data are not checked for normal distribution, statistical analyses of radiotracer binding in the whole brain were analyzed using Mann Whitney nonparametric test with U, *p* and median values are reported. All statistical analyses were performed using Graphpad Prism version 9.1.0. Graphs were made using Graphpad Prism version 9.1.0. A *p*-value less than 0.05 was considered statistically significant.

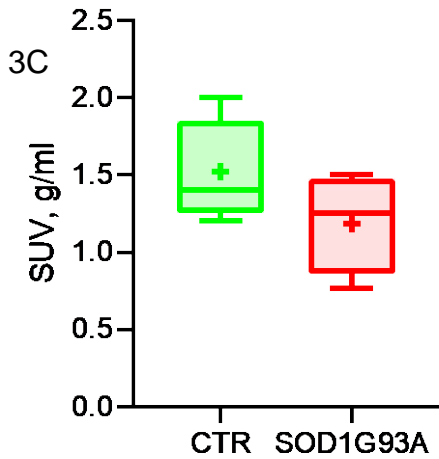
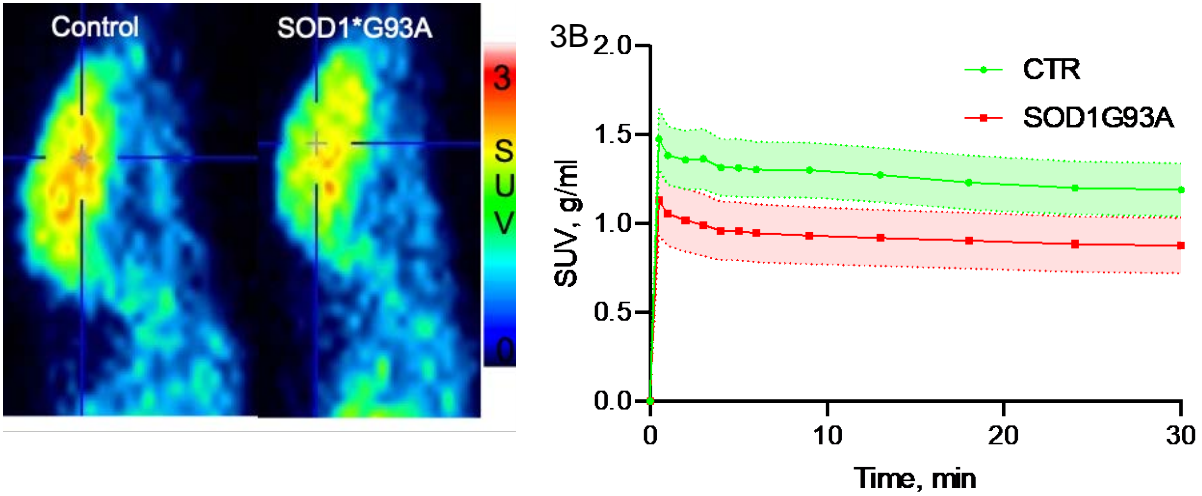
### Results





Initially, we examined the binding of [ $^{11}\text{C}$ ]MPC-6827 in transgenic rTg4510 mice and their wild type littermates (Figure 2). We performed scans in 9-month-old rTg4510 mice due to literature evidence of the significant loss of dendritic spines and the progressive loss of neurons at this age [18]. MicroPET analyses show excellent BBB penetration and retention of [ $^{11}\text{C}$ ]MPC-6827 in rTg4510 mice and age matched controls ( $n = 5$ ) (Figure 2A). Time activity curves (TACs) show brain peak uptake at approximately 2 minutes followed by a washout of [ $^{11}\text{C}$ ]MPC-6827 from the brain. The whole brain uptake of the radiotracer is slightly less in rTg4510 mice group compared to wild type control group (Figure 2B). SUV data show lower binding of tracer (~15%) in whole brain rTg4510 group than wild type mice group (Figure 2C). Statistical analyses of whole brain SUV data show small effect size of radiotracer binding between rTg4510 (median = 2.38,  $n = 5$ ) and wild type controls (median = 2.68,  $n = 5$ ) (Mann Whitney test,  $U = 6$ ,  $p = 0.22$ ).

Subsequently, we examined the binding of [ $^{11}\text{C}$ ]MPC-6827 in ALS mice model SOD1\*G93A and control groups (Figure 3). MicroPET imaging in 2-month-old SOD1\*G93A mice shows lower binding of [ $^{11}\text{C}$ ]MPC-6827 in whole brain compared to control littermates (Figure 3A). TACs and SUVs also demonstrate ~20% lower binding of tracer in transgenic mice compared to controls (Figures 3B and 3C). Statistical analyses of SUVs show a drift towards lower binding of [ $^{11}\text{C}$ ]MPC-6827 in whole brain SUV data between transgenic (median = 1.4,  $n = 5$ ) and control groups (median = 1.25,  $n = 5$ ) (Mann Whitney test,  $U = 7$ ,  $p = 0.31$ ).



## Discussion

NDs strike primarily in mid-to-late life and are one of the incurable human diseases recognized as major causes of death and disability [20-23]. A biomarker is urgently needed for diagnosing NDs prior to symptom development to aid prevention or to monitor disease progression. MTs, one of the fundamental components of cytoskeleton are implicated in the pathogenesis of several NDs, and MT loss in neurons is directly connected to neurodegeneration [4-6]. Our team recently developed [ $^{11}\text{C}$ ]MPC-6827 as the first brain-penetrating MT radiotracer, that exhibits specific binding in rodent brain [15-17]. We selected rTg4510 mice for preclinical imaging due to the overexpression of pathological human tau and it develops neurofibrillary tangles (NFTs) in a progressive and age-related pattern [18]. This is accompanied by deficits in synaptic functioning

including long-term potentiation (LTP), brain atrophy and learning/memory behaviors [18]. It is one of the most robust and well validated mouse models of AD and FTD tau pathology. Among the biomarkers of ALS, significant loss of MT is reported in postmortem ALS brain [10-12]. Pharmacological stabilization of the MT network offers an attractive therapeutic strategy in ALS. Among the transgenic animal models, SOD1\*G93A is the oldest and most widely used model of ALS including preclinical imaging with PET [19]. The SOD1\*G93A model has demonstrated degeneration of the neuromuscular junction at around 40 to 50 days of age and before the onset of symptoms. Gliosis was found before the onset of symptoms and increased in intensity over time along with motor impairment and activated microglia during the onset of symptoms, around age of 3 months. Up to 50% loss of motor cortex neurons in the cervical and lumbar segments of the spinal cord at the end stage (~age of 120 days) was also observed in SOD1\*G93A [12,19]. Furthermore, stabilization of MT dynamics is established in SOD1\*G93A mice and treatment with MTAs caused improvement in neuropathology and behavioral symptoms, supporting the use of this animal model for PET studies of MT [12].

The data presented in this manuscript report the first preclinical evaluation of MT targeted PET tracer in mouse models of AD/FTD and ALS. Both models demonstrate lower binding of [<sup>11</sup>C]MPC-6827 radiotracer compared to their age-matched control littermates. MicroPET experiments in both transgenic and control mice exhibit >30% variations of SUV within the groups. One pair of animals per each transgenic and control group exhibited very low uptake (SUV: 0.1-0.3), probably due to the low brain retention of injected doses of [<sup>11</sup>C]MPC-6827. These animals were excluded from the study. One pair shows higher SUV for transgenic mouse group compared to controls and is included in the outcome measurements.

## **Conclusions**

In summary, our pilot preclinical imaging studies show a lower binding of MT PET tracer [<sup>11</sup>C]MPC-6827 in ALS and AD/FTD mouse models compared to corresponding controls. The above findings support previous reports of loss of MTs in AD/FTD and ALS brain [4-6]. Experiments comparing metabolite corrected arterial input function data and

larger sample size and comparison with in vitro tubulin levels of imaged animals may provide further verification of these results.

### **Funding source**

This work was funded by NCATS UL1TR001873 (Reilly) Irving Institute/CTSA Translational Therapeutics Accelerator.

### **Conflict of interest statement**

The authors declare no conflict of interest.

### **Author contributions**

J.S.D.K. conceived the idea. J.S.D.K. and A.M designed the experiments. J. S. D. K, A.M, P.C., J.P, S. I., and J.C. performed the experiments. J.S.D.K, and A.M. performed all analyses. J.S.D.K, A.M, and A.M. analyzed and interpret the data. J.S.D.K drafted the manuscript. The manuscript was written through contributions of all authors and all authors have given approval to the final version of the manuscript

### **References**

1. Fan HC, Chi CS, Lee YJ, Tsai JD, Lin SZ, Harn HJ. The Role of Gene Editing in Neurodegenerative Diseases. *Cell Transplant*. 2018;27(3):364-378.
2. Sheikh S, Safia, Haque E, Mir SS. Neurodegenerative Diseases: Multifactorial Conformational Diseases and Their Therapeutic Interventions. *J Neurodegener Dis*. 2013; 2013:563481.
3. Nery TGM, Silva EM, Tavares R, Passetti F. The Challenge to Search for New Nervous System Disease Biomarker Candidates: the Opportunity to Use the Proteogenomics Approach. *J Mol Neurosci*. 2019; 67(1):150-164.
4. Varidaki A, Hong Y, Coffey ET. Repositioning Microtubule Stabilizing Drugs for Brain Disorders. *Front Cell Neurosci*. 2018;12, 226.
5. Brunden KR, Lee VM, Smith AB 3rd, Trojanowski JQ, Ballatore C. Altered microtubule dynamics in neurodegenerative disease: Therapeutic potential of microtubule-stabilizing drugs. *Neurobiol Dis*. 2017;105, 328-335.

6. Matamoros AJ, Baas PW. Microtubules in health and degenerative disease of the nervous system. *Brain Res Bull.* 2016;126(Pt 3):217-225.
7. Sleight JN, Rossor AM, Fellows AD, Tosolini AP, Schiavo G. Axonal transport and neurological disease. *Nat Rev Neuol.* 2019;15: 691-703.
8. Salvadores N, Sanhueza M, Manque P, Court FA. Axonal Degeneration during Aging and Its Functional Role in Neurodegenerative Disorders. *Front Neurosci.* 2017; 11:451.
9. Liu X-A, Rizzo V, Puthanveetil SV. Pathologies of axonal transport in neurodegenerative diseases. *Transl Neurosci.* 2012; 3(4): 355–372.
10. Oberstadt M, Claßen J, Arendt T, Holzer M. TDP-43 and Cytoskeletal Proteins in ALS. *Mol Neurobiol.* 2017; 55(4): 3143-3153.
11. Clark JA, Yeaman EJ, Blizzard CA, Chuckowree JA, Dickson TC. A Case for Microtubule Vulnerability in Amyotrophic Lateral Sclerosis: Altered Dynamics During Disease. *Front Cell Neurosci.* 2016;10: 204.
12. Fanara P, Banerjee J, Hueck RV, Harper MR, Awada M, Turner H, Husted KH, Brandt R, Hellerstein MK. Stabilization of hyperdynamic microtubules is neuroprotective in amyotrophic lateral sclerosis. *J Biol Chem.* 2007; 282(32):23465-72.
13. Dubey J, Ratnakaran N, Koushika SP. Neurodegeneration and microtubule dynamics: death by a thousand cuts. *Front Cell Neurosci.* 2015; 9:343.
14. Van der Veldt AAM, Lammertsma AA. In Vivo Imaging as a Pharmacodynamic Marker. *Clin Cancer Res.* 2014; 20 (10):2569-2577.
15. Kumar JSD, Solingapuram SKK, Prabhakaran J, Oufkir HR, Ramanathan G, Whitlow CT et al. Radiosynthesis and In vivo evaluation of [11C]MPC-6827, the first brain penetrant microtubule PET ligand. *J Med Chem.* 2018; 61(5):2118-2123.
16. Kumar JSD, Prabhakaran J, Damuka N, Hines JW, Norman S, Meghana DM et al. In vivo comparison of N-11CH3 vs O-11CH3 radiolabeled microtubule targeted PET ligands. *Bioorg Med Chem Let.* 2010; 30(2): 126785.

17. Kumar JSD, Molotkov A, Salling MC, Carberry P, Prabhakaran J, Castrillon J, Mintz A. In vivo evaluation of a microtubule PET ligand, [(11)C]MPC-6827, in mice following chronic alcohol consumption. *Pharmacol Rep.* 2022; 74(1):241-247.
18. <https://www.alzforum.org/research-models/rtgtaup30114510> ALZFORUM website accessed on October 4, 2021.
19. <https://www.alzforum.org/research-models/sod1-g93a-hybrid-g1h> ALZFORUM website accessed on October 4, 2021.
20. Checkoway H, Lundin JI, Kelada SN. Neurodegenerative diseases. *IARC Sci Publ.* 2011;(163):407-19.
21. Erkinen MG, Kim MO, Geschwind MD. Cold Spring Harb Perspect Biol. *Clinical Neurology and Epidemiology of the Major Neurodegenerative Diseases.* 2018; 10(4):a033118.
22. Heemels MT. Neurodegenerative diseases. *Nature.* 2016; **539**, 179.
23. Picher-Martel V, Valdmanis PN, Gould PV, Julien JP, Dupre N. From animal models to human disease: a genetic approach for personalized medicine in ALS. *Acta Neuropathol Commun.* 2016; 4(1):70.

## Figure captions

1. Figure 1. Chemical structure of [<sup>11</sup>C]MPC-6827
2. Figure 2. A. Representative static (0-55 minutes) microPET images of [<sup>11</sup>C]MPC-6827 scan in rTg4510 (right) and control mice (left) ; B. Average time activity curves of [<sup>11</sup>C]MPC-6827 in rTg4510 (red) and wild type littermates (green). Values are reported as the mean ± SEM from five pairs of mice per group; C. Standardized uptake values (SUV) of [<sup>11</sup>C]MPC-6827 in rTg4510 (red) and wild type mice (green). Whole brain SUV values show a trend of lower binding but were not statistically significant different between rTg4510 (median = 2.38, n = 5) and wild type controls (median = 2.68, n =5) groups (Mann Whitney test, U=6,  $p = 0.22$ ).
3. Figure 3. A. Representative static (0-30 minute) microPET images of [<sup>11</sup>C]MPC-6827 in SOD1\*G93A (right) and control mice (left); B. Average time activity curves of [<sup>11</sup>C]MPC-6827 in SOD1\*G93A (red) and control mice (green). Values are reported as the mean ± SEM from five pairs of mice per group; C. Standardized uptake values of [<sup>11</sup>C]MPC-6827 in SOD1\*G93A (red) and control mice (green). Whole brain SUV values show a drift of lower binding of tracer but were not statistically significantly different between SOD1\*G93A (median = 1.4, n = 5) and wild type controls (median = 1.25, n = 5) groups (Mann Whitney test, U= 7,  $p = 0.31$ ).